A Numerical Analysis for Tsunamis Due to Falling Rigid Bodies

Taro Kakinuma

Graduate School of Science and Engineering, Kagoshima University

1. Introduction

Tsunamis can be triggered by not only submarine earthquakes but also by landslides. In 1792, the tsunamis due to a landslide, or a sector collapse, at Mt. Mayu, Japan, traveled over the Ariake Sea, resulting in a runup on the opposite shore[1]. Such tsunamis are not necessarily generated only by soil or rocks: an excursion ship could be hit by tsunamis due to a partial collapse of glacier near a coast on Svalbard Islands, Norway[2]. These tsunamis are generated through an interaction between water motion and falling bodies, such that the tsunami generation process is rather complicated. In the present study, we will investigate several fundamental characteristics of tsunami generation caused by a landslide, or a sector collapse, on the basis of vertically two-dimensional results, obtained through a numerical simulation based on a Lagrangian method, where the falling body is assumed to be a rigid mass, or a group of rigid bodies, which moves down a slope with a constant gradient.

2. Numerical method and conditions

Tsunami generation due to a landslide or a sector collapse is simulated using a moving particle semi-implicit (MPS) model[3], where the water surface level is determined using the spatial gradient of particle-number density, to inhibit pressure disturbance at the water surface. The interparticle distance is 0.005 m in the present cases. No turbulence model is utilized for fluid motion, and both fluid viscosity and surface tension are neglected for simplicity.

Figure 1 shows the target domain inside a water basin with a slope, where the gradient of the slope is 45°. The distance between the starting point of the slope and the offshore wall is 3.00 m, and the still water depth off the slope is uniformly 0.09 m or 0.245 m. The origin of the coordinate axes is at the shoreline in the still water condition. The horizontal offshore direction is the positive direction of the x-axis, while the upward direction is the positive direction of the z-axis.

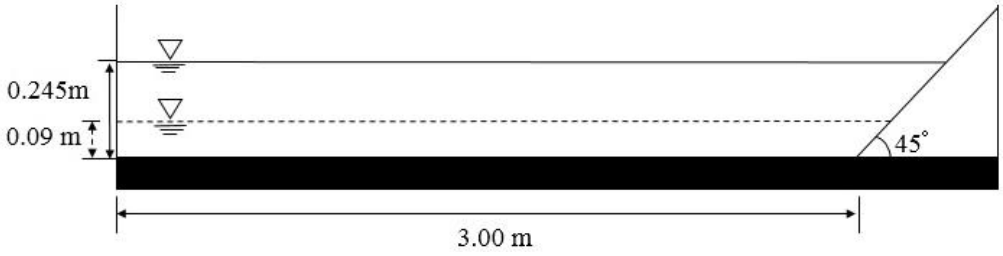

Fig. 1. The target domain inside a water basin with a slope.

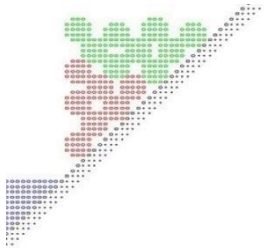

Fig. 2. A sketch of the large circles at the initial condition.

The release of objects, stacked on the slope, generates tsunamis, where the falling objects are assumed to be rigid bodies as follows:

(1) Large circle: The diameter of large circles is 2.0 cm. A large circle consists of 21 rigid particles.
(2) Small circle: The diameter of small circles is 0.5 cm. A small circle consists of 4 rigid particles.
(3) Right triangle: A right triangle consists of 276 rigid particles.
(4) Rectangle: A rectangle consists of 276 rigid particles.

The fluid density is 1,000 kg/m^3, while the density of the rigid particles is 2,600 kg/m^3. Both the elasticity and the plasticity of the falling bodies are neglected for simplicity.

3. Tsunamis caused by falling large circles

As shown in Fig. 2, 16 large circles are arranged on the slope at the initial time t = 0.0 s. Figure 3 shows the numerical simulation result, where the uniform still water depth off the slope, h, is 0.09 m.

The water surface displacements at x = 0.6 m and 2.15 m are shown in Fig. 4, where x denotes the distance from the shoreline in the still water condition. In this paper, the results for water surface displacements are moving average values with a sampling interval of 0.01 s. The tsunami height is defined as the maximum value of water surface displacement at each point. According to Fig. 4(a), the tsunami height at x = 0.6 m is 0.072 m when h = 0.09 m, and 0.068 m when h = 0.245 m, such that the difference between them is small, that is, the tsunami height, immediately after the great circles enter the water, does not depend much on the still water depth. Conversely, according to Fig. 4(b), the tsunami height at x = 2.15 m is 0.066 m when h = 0.09 m, and 0.032 m when h = 0.245 m, such that the tsunami-height reduction rate differs greatly for the two cases, for the reduction in the tsunami height is suppressed owing to shallowing in the former with the shallower offshore still water depth.

4. Tsunamis caused by falling small circles

As indicated in Fig. 5, 66 rigid small circles are placed on the slope at the initial time t = 0.0 s. Both the total mass, and the vertical position of the center of gravity at t = 0.0 s, of all the small circles are equal to those of all the large circles shown in Fig. 2. Shown in Fig. 6 are the water surface displacements at x = 0.6 m and 2.5 m. According to Fig. 6(a), the tsunami height at x = 0.6 m is 0.061 m when h = 0.09 m, and 0.046 m when h = 0.245 m, such that there is a difference in the tsunami height, immediately

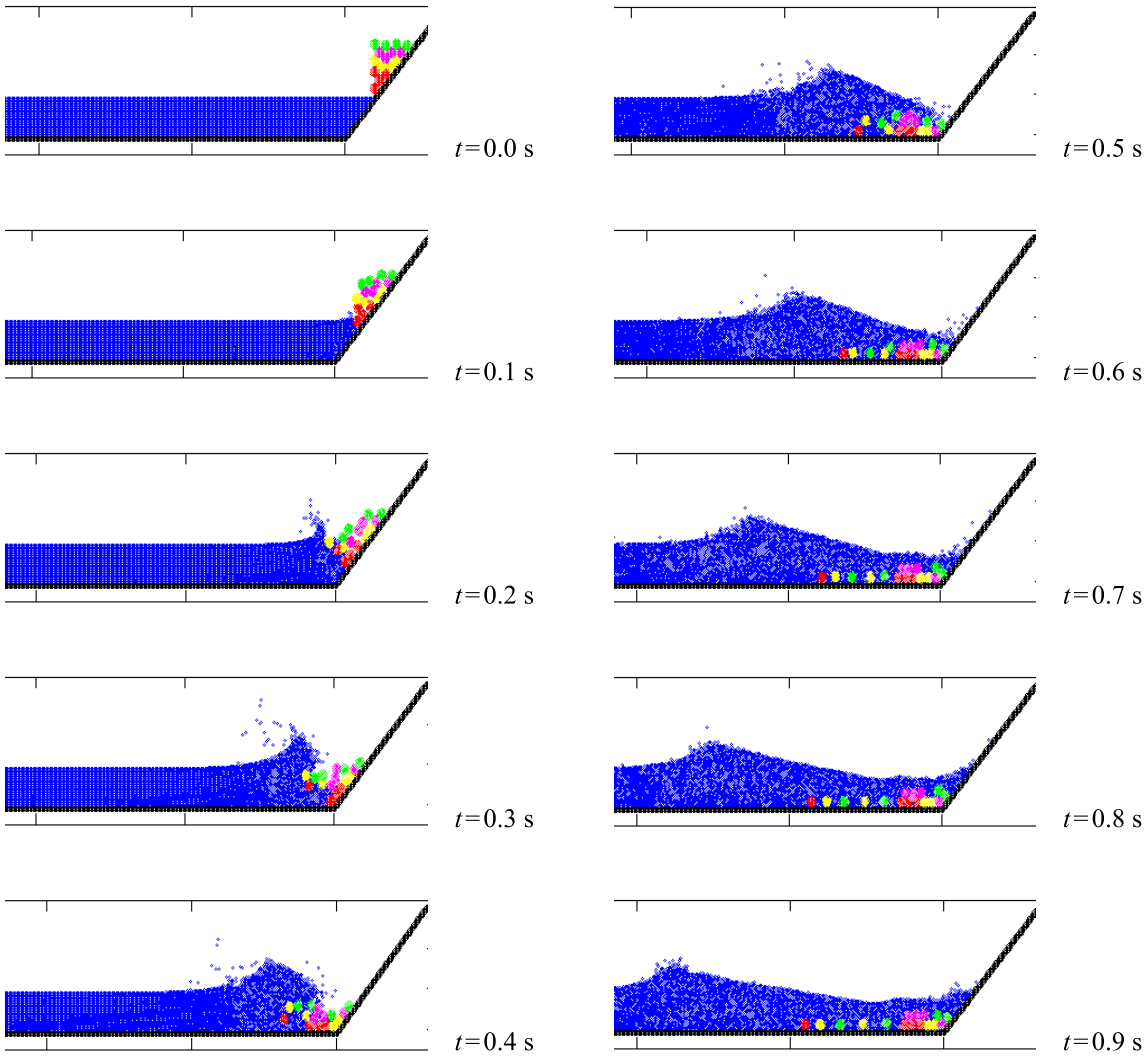

Fig. 3. The numerical result of the tsunamis caused by the falling large circles, where h = 0.09 m.

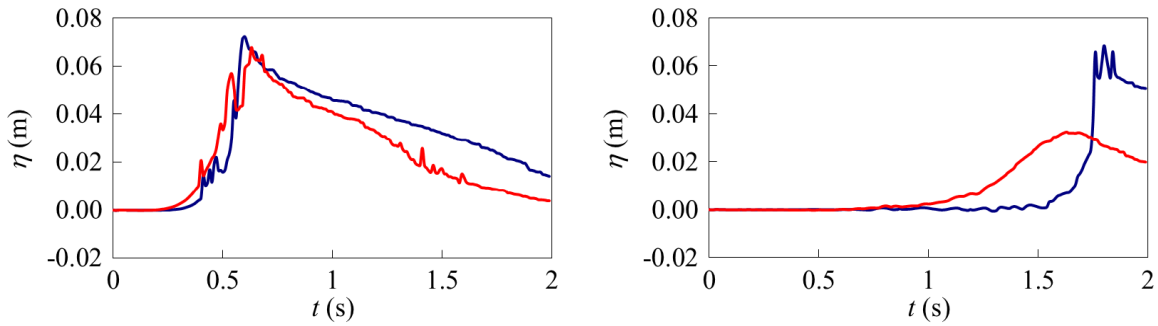

(a) x=0.6 m (b) x=2.15 m

Fig. 4. The water surface displacements due to the falling large circles. The blue lines represent the water surface displacements when h = 0.09 m, and the red lines when h = 0.245 m.

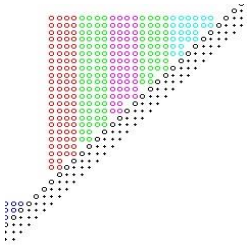

Fig. 5. A sketch of the small circles at the initial condition.

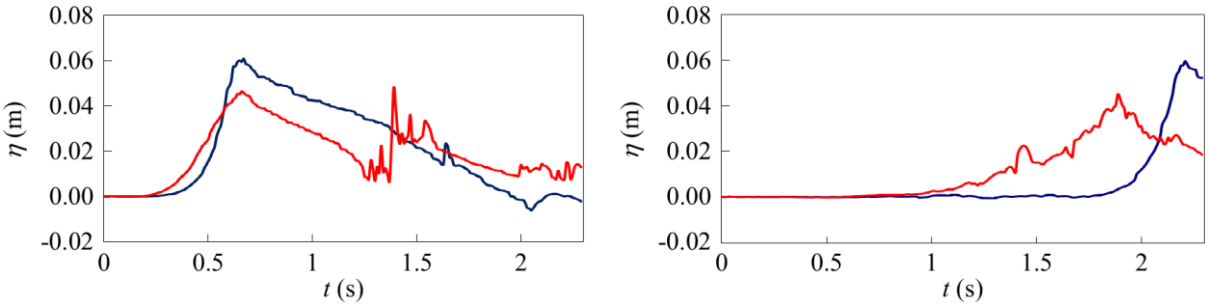

(a) $x = 0.6$ m (b) $x = 2.5$ m

Fig. 6. The water surface displacements due to the falling small circles. The blue lines represent the water surface displacements when $h = 0.09$ m, and the red lines when $h = 0.245$ m.

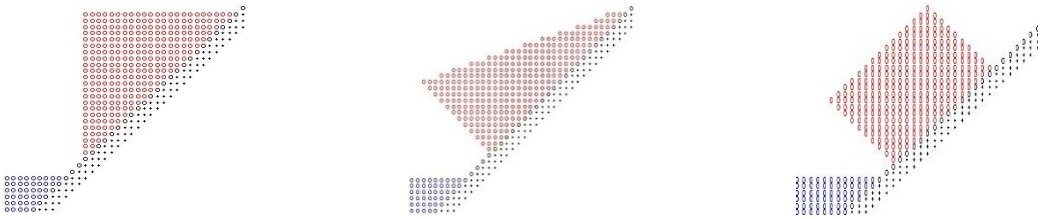

(a) a right-angled isosceles triangle (b) a right triangle (c) a rectangle

Fig. 7. Sketches of the rigid masses at the initial conditions.

after the small circles enter the water, where the tsunami height increases as the offshore still water depth is shallower. According to Figs. 4(a) and 6(a), the tsunami height, immediately after the rigid bodies enter the water, is larger when the falling bodies are the large circles than when those are the small circles. Conversely, according to Fig. 6(b), the tsunami height at $x = 2.5$ m is 0.060 m when $h = 0.09$ m, and 0.045 m when $h = 0.245$ m, such that the reduction rate of tsunami height is smaller for the falling small circles than for the falling large circles.

5. Tsunamis caused by a falling right triangle or a falling rectangle

As illustrated in Fig. 7, the falling body is a right-angled isosceles triangle with an equilateral length of 0.11 m, a right triangle, or a rectangle, where both their area, and their vertical position of the center of gravity at $t = 0.0$ s, are equal.

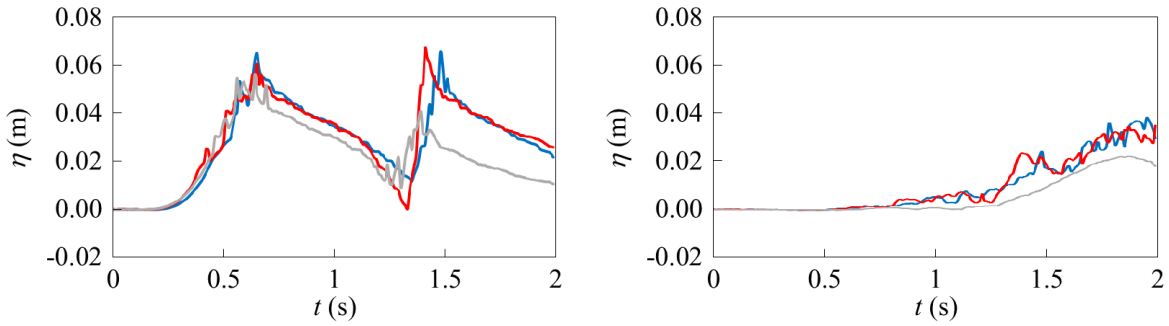

(a) x = 0.6 m (b) x = 2.5 m

Fig. 8. The water surface displacements due to the falling rigid masses, where h = 0.245 m. The blue lines represent the water surface displacements due to the right-angled isosceles triangle; the red lines due to the right triangle; the gray lines due to the rectangle.

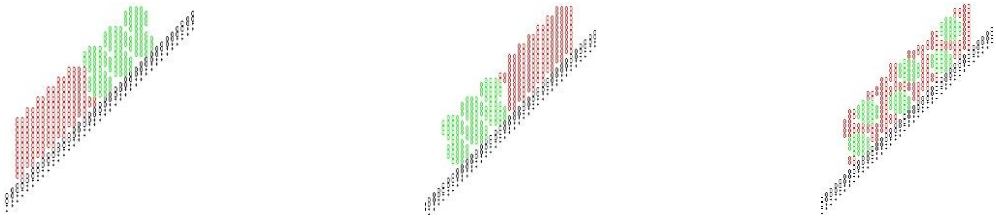

(a) The large circles are on the onshore side. (b) The large circles are on the offshore side. (c) The large and small circles are mixed.

Fig. 9. Sketches of the rigid bodies, including both the large and small circles, at the initial conditions.

Figure 8 shows the water surface displacements at x = 0.6 m and 2.5 m, where the offshore still water depth h is 0.245 m. The tsunami height of the first wave, immediately after the rigid mass enters the water, is almost the same regardless of the rigid-mass shape. The tsunami height of the second wave, however, is smaller than that of the first wave only in the case of the rectangle. In all the cases, the second wave shows a relatively large wave height, for water cannot flow into the area occupied by the rigid mass after landing. At the location x = 2.5 m, the tsunami height of the first wave has been greatly reduced in all the cases, such that the reduction rate of tsunami height is larger than that for the cases where the falling rigid bodies are the circles.

6. Tsunamis caused by falling rigid bodies including both large and small circles

As shown in Fig. 9, both the large and small circles are loaded at the initial time. Figure 10 shows the water surface displacements at x = 0.6 m, where the offshore still water depth h is 0.09 m. Although there is no significant difference in the tsunami height for these cases, immediately after the falling bodies plunge into the water, the reduction rate of water level at this location is larger when the large circles are also stacked on the offshore side at the initial condition.

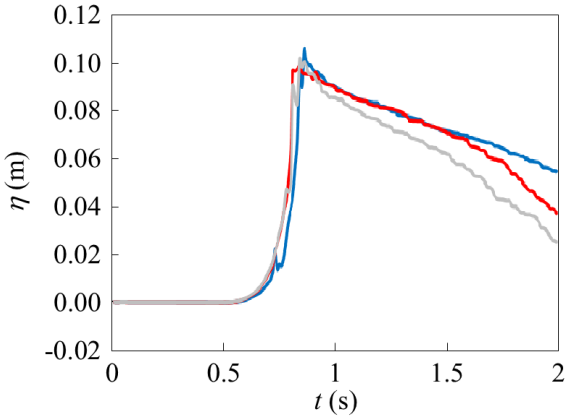

Fig. 10. The water surface displacements at $x = 0.6$ m, due to the falling rigid bodies including both the large and small circles, where $h = 0.09$ m. The blue line represents the water surface displacement when the large circles are initially arranged on the onshore side; the red line when the large circles are initially stacked on the offshore side; the gray line when the large and small circles are mixed at the initial condition.

7. Tsunamis running up the slope where the landslide has occurred

In general, when a landslide occurs in water, the effect of the density ratio is smaller than when a landslide occurs on land, for the surrounding of the collapsed body is water, such that the falling speed of the collapsed body is slow, and the tsunami is unlikely to grow (Kakinuma, 2016). It is necessary, however, to consider the tsunami component that travels toward the shore and runs up on land, when tsunamis are caused by a nearshore landslide whether the landslide begins above or below the sea level. Figure 11 shows the numerical simulation results at $t = 0.8$ s, when the height of the upstream end becomes large on the slope, where the falling mass is placed on the slope above the still water level as shown in Fig. 7. The offshore still water depth h is 0.245 m. When the rigid mass is the right-angled isosceles triangle, the right triangle, and the rectangle, as shown in Fig. 7, the runup height z_{up} is 0.11 m, 0.094 m, and 0.047 m, respectively, such that if the offshore still water depth h is 10.0 m, with a length scale of 0.0245, the runup height z_{up} is around 4.5 m, 3.8 m, and 1.9 m, respectively. These values are the runup heights at which wooden structures can be damaged.

8. Conclusions

The tsunamis generated by the falling rigid bodies were numerically simulated using the MPS model in the vertical two dimensions. The tsunami height, immediately after the large circles entered the water, did not depend much on the offshore still water depth, while the tsunami-height reduction was suppressed, when the offshore still water depth is shallower. Conversely, the tsunami height, immediately after the small circles entered the water, increased as the offshore still water depth was shallower. Both the tsunami height, immediately after the falling bodies entered the water, and the reduction rate of tsunami height, were larger for the large circles than for the small circles. Furthermore, in the cases where the falling bodies included both the large and small circles, the reduction rate of the

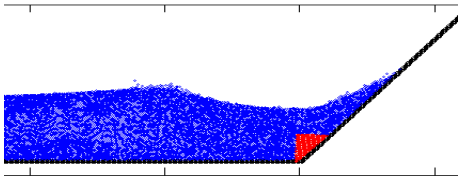

(a) The right-angled isosceles triangle

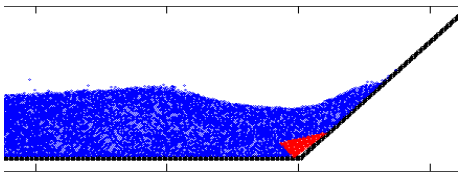

(b) The right triangle

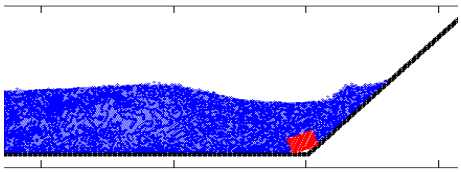

(c) The rectangle

Fig. 11. The numerical simulation results at $t = 0.8$ s, where the falling rigid masses at the initial time $t = 0.0$ s are shown in Fig. 7; $h = 0.245$ m.

water level near the wave source was larger, when the large circles are also stacked on the offshore side at the initial condition.

The tsunami height of the first wave, immediately after the rigid masses entered the water, was almost the same regardless of the rigid-mass shape. The tsunami height of the second wave was larger than that of the first wave in the cases of the right-angled isosceles triangles and the right triangles. The reduction rate of tsunami height for the rigid masses was larger than that for the circles. In the cases where the falling body was one of the rigid masses, a tsunami component traveling toward the shore and running up the slope was confirmed.

Acknowledgments

Sincere gratitude is extended to Dr. Tsunakiyo Iribe, University of the Ryukyus, who allowed me to apply his computational program, based on the MPS method. This work was supported by the Research Institute for Mathematical Sciences, an International Joint Usage/Research Center located in Kyoto University. I also express my gratitude to Ms. Manami Higashi, Ms. Aya Oyama, and Mr. Ryo Sawada, who contributed to the numerical simulation, when they were student members of our laboratory.

References

1) Togashi, H. and Hirayama, Y. Hydraulic experiment on reappearance of the Ariake-kai tsunami in 1792, Proc. IUGG/IOC Int. Tsunami Symp. (Tsunami ’93), pp. 741-754, 1993.

2) Marchenko, A. V., Morozov, E. G. and Muzylev, S. V.: A tsunami wave recorded near a glacier front, Nat. Hazards Earth Syst. Sci., Vol. 12, pp. 415-419, 2012.

3) Iribe, T. and Nakaza, E.: An improvement of accuracy of the MPS method with a new gradient calculation model, J. JSCE, B2 (Coastal Eng.), Vol. 67, No. 1, pp. 36-48, 2011 (in Japanese with an English abstract).

4) Kakinuma, T.: Tsunami generation due to a landslide or a submarine eruption, In: Tsunami (ed. Mokhtari, M.), InTech, pp. 35-58, 2016.